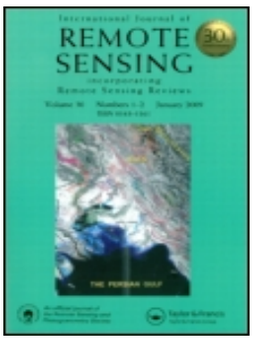

International Journal of Remote Sensing

ISSN: 0143-1161 (Print) 1366-5901 (Online) Journal homepage: http://www.tandfonline.com/loi/tres20

Comparing MODIS and MERIS spectral shapes for cyanobacterial bloom detection

T.T. Wynne , R.P. Stumpf & T.O. Briggs

To cite this article: T.T. Wynne , R.P. Stumpf & T.O. Briggs (2013) Comparing MODIS and MERIS spectral shapes for cyanobacterial bloom detection, International Journal of Remote Sensing, 34:19, 6668-6678, DOI: 10.1080/01431161.2013.804228

To link to this article: http://dx.doi.org/10.1080/01431161.2013.804228

International Journal of Remote Sensing, 2013
Vol. 34, No. 19, 6668–6678, http://dx.doi.org/10.1080/01431161.2013.804228

Taylor & Francis
Taylor & Francis Group

Comparing MODIS and MERIS spectral shapes for cyanobacterial bloom detection

T.T. Wynne[a]*, R.P. Stumpf[a], and T.O. Briggs[b]

[a]*NOAA National Centers for Coastal Ocean Science, Silver Spring, MD 20190, USA;*
[b]*CSS-Dynamac, Silver Spring, MD 20190, USA*

(*Received 4 February 2013; accepted 7 May 2013*)

A spectral shape algorithm applied to Medium Resolution Imaging Spectrometer (MERIS) imagery has detected cyanobacterial blooms, with extensive examples in Lake Erie. The detection algorithm uses an approximation of the second derivative as a measure of spectral shape around the 681 nm band $S_{2d}(681)$. With the end of the MERIS mission on 8 April 2012, an analogue was developed for the Moderate Resolution Imaging Spectroradiometer (MODIS) to continue monitoring for these blooms. The MODIS analogue uses the standard ρ_s (Rayleigh-corrected reflectance) to determine $S_{2d}(678)$, which is computationally equivalent to the negative of the MODIS fluorescent line height (FLH). A comparison was made of the two products from image pairs during a period of relatively severe blooms of cyanobacteria (2008–2011). When the MODIS bands do not saturate due to surface scums from high cyanobacteria biomass or conditions of glint or dense aerosols, the algorithms produce comparable results with a linear transform of the MODIS $S_{2d}(678)$. The results indicate that MODIS can be used to monitor these blooms. Dense cyanobacteria blooms will produce negative FLH showing a limitation of FLH for bloom detection. The $S_{2d}(678)$ offers a tool to support monitoring for dense algal blooms.

1. Introduction

Lake Erie is one of the world's largest lakes and the fourth largest of the Laurentian Great Lakes (Figure 1). In the 1970s, the lake experienced extensive cyanobacterial blooms, including *Microcsystis aeruginosa* (henceforth *Microcystis*). However, the blooms diminished when phosphorus reduction strategies were successfully implemented in the 1980s. *Microcystis* blooms reappeared in 1995 and have been present to a varying degree every year since (Budd et al. 2001; Brittain et al. 2000; Vanderploeg et al. 2001; Stumpf et al. 2012). The reemergence of the blooms in the 1990s coincides with the emergence of invasive mussels of the genus *Dreissena*. These mussels have been hypothesized to play a role in the reintroduction of cyanobacterial blooms through selective rejection of toxic *Microcystis* (Vanderploeg et al. 2001; Juhel et al. 2006).

The use of ocean colour remote sensing is advantageous as it allows a synoptic view at the high temporal resolution (up to one image per day) needed to address bloom dynamics, growth, and senescence. Imagery from the Medium Resolution Imaging Spectrometer (MERIS) aboard the European Space Agency's (ESA's) ENVISAT-1 spacecraft can

*Corresponding author. Email: timothy.wynne@noaa.gov

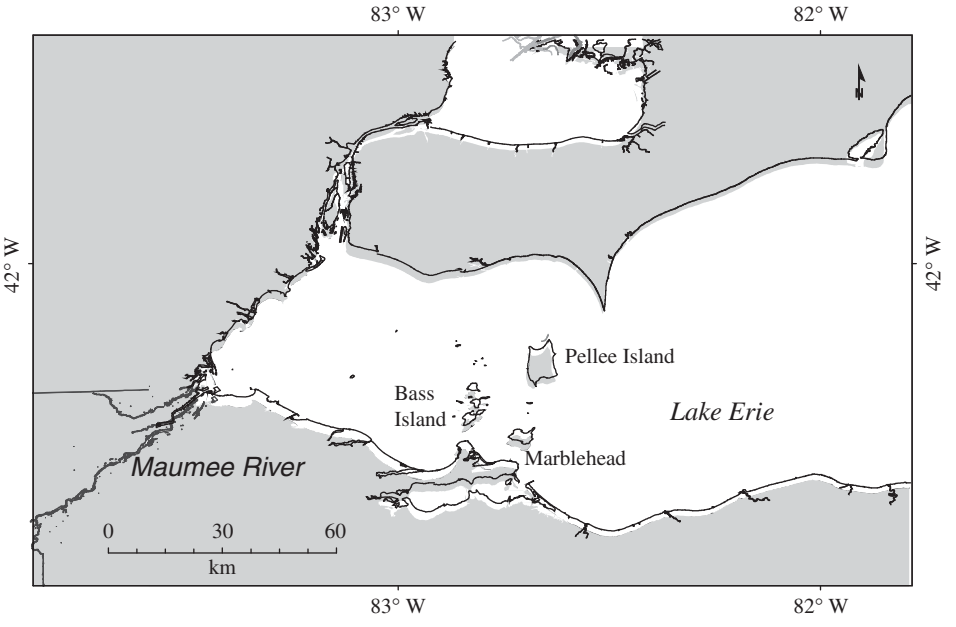

Figure 1. Map indicating the study area. All other images in subsequent figures cover the same area.

identify these blooms (Wynne et al. 2008, 2010), and has been used to routinely monitor the blooms to support management needs (Wynne et al. 2013). On 8 April 2012, ESA lost communication with ENVISAT-1, and after repeated attempts to establish communication with the satellite failed, ESA concluded the ENVISAT-1 mission on 9 May 2012. MERIS imagery was an integral part of a harmful algal bloom (HAB) forecast that was distributed weekly during the bloom season (nominally 1 June through 31 October) (Wynne et al. 2013). Forecasts were distributed via email to approximately 500 subscribers and posted on the internet (archives available at: http://www2.nccos.noaa.gov/coast/lakeerie/bulletin/).

Derivatives are robust methods of analysing remote sensing data in the presence of challenging atmospheric conditions (Philpot 1991; Gower, Doerffer, and Borstad 1999; Stumpf and Werdell 2010). Second derivatives, which capture the spectral curvature, are effective for indicating pigments, including chlorophyll (Lubac et al. 2008; Shi et al. 2007). A form of this computation for satellite data has appeared under a variety of names, changing with the central band and application, including the maximum chlorophyll index (MCI, Gower), the fluorescent line height (FLH) (Letelier and Abbot 1996), and the cyanobacteria index (CI, Wynne et al. 2008).

MERIS has been widely used to delineate cyanobacterial blooms (Wynne et al. 2008; Binding, Greenberg, and Bukata 2011; Ruiz-Verdú et al. 2008; Kutser et al. 2006). To establish routine monitoring in the presence of glint, problematic atmospheric correction, and other interferences, Wynne et al. (2008) applied the CI spectral shape algorithm that uses a second derivative approach around the MERIS 681 nm band (using adjacent 665 nm, 681 nm, and 709 nm bands). The results have been applied for routine monitoring of Lake Erie for several years (Wynne et al. 2013). With the loss of MERIS data on 8 April 2012, the need for another option became apparent. The Moderate Resolution Imaging Spectroradiometer (MODIS) has similar bands centred at 678 nm (667 nm, 678 nm, and 754 nm) that may allow application of an equivalent algorithm. As the Ocean Land Colour

Imager (OLCI) on the planned Sentinel-3 satellite will have an equivalent band set to MERIS, using MODIS to cover the gap from MERIS to OLCI would benefit analysis of cyanobacteria trends in the lake. When applied to MODIS, the CI would produce the negative of the FLH (a positive CI would correspond to a negative value for FLH). The results described here indicate that, as with MERIS, these intense blooms can be identified by an approximation of the second derivative around 681 nm.

2. Methods

Level 1 MODIS Aqua imagery was obtained from the National Aeronautics and Space Administration (NASA). These images were then processed through the Naval Research Laboratory's (NRL's) Automated Processing System (APS version 4.0.14) using standard NASA processing (NASA 2012) and mapped using the nearest neighbour method. From this point the spectral shape around the 678 nm band was calculated by

$$S_{2d}(678) = \rho_s(678) - \rho_s(667) - \{\rho_s(748) - \rho_s(667)\}\frac{(678-667)}{(748-667)}, \quad (1)$$

where S_{2d} is the second derivative (Stumpf and Werdell 2010), ρ_s is the Rayleigh-corrected reflectance, and 667, 678, and 748 are numeric values from the wavelengths used (expressed in nm). The use of S_{2d} allows potential data retrieval in conditions where the atmospheric correction might fail, such as areas of high glint or aerosols (Gower and King 2007). The standard cloud flagging procedure was used to mask clouds (L2 flags; NASA 2010).

MERIS L2 reflectance imagery from the second reprocessing (Montagner 2001) was acquired from ESA. The reflectance (R) data were used to calculate the spectral shape by Equation (2):

$$S_{2d}(681) = R(681) - R(665) - \{R(709) - R(665)\}\frac{(681-665)}{(709-665)}. \quad (2)$$

The negative of the S_{2d} was then calculated to retrieve the MODIS and MERIS CI from methods proposed in Wynne et al. (2010),

$$CI_{MODIS} = -S_{2d}(678), \quad (3)$$

$$CI_{MERIS} = -S_{2d}(681). \quad (4)$$

The ρ_s is the irradiance reflectance or albedo (reflectance (in sr^{-1}) multiplied by π sr), whereas R is the water remote sensing reflectance (units of sr^{-1}). Accordingly, $S_{2d}(678)$ and CI_{MODIS} are dimensionless, while R, $S_{2d}(681)$, and CI_{MERIS} have units of sr^{-1}.

Figure 2 shows examples of the spectra used for the shape algorithm from both MODIS and MERIS. Illustrated are four different spectra from a 'high' value (CI of 0.01136 and 0.00835, MODIS and MERIS, respectively). A 'medium' value (CI of 0.00174 and 0.00149), and a 'low' value (CI of 0.00058 and 0.00043). Additionally, an 'Absent' value was included, absent being a negative CI, indicative of the absence of a cyanobacterial bloom (CI values of –0.00028 and –0.00025). The spectra show that high CI values occur

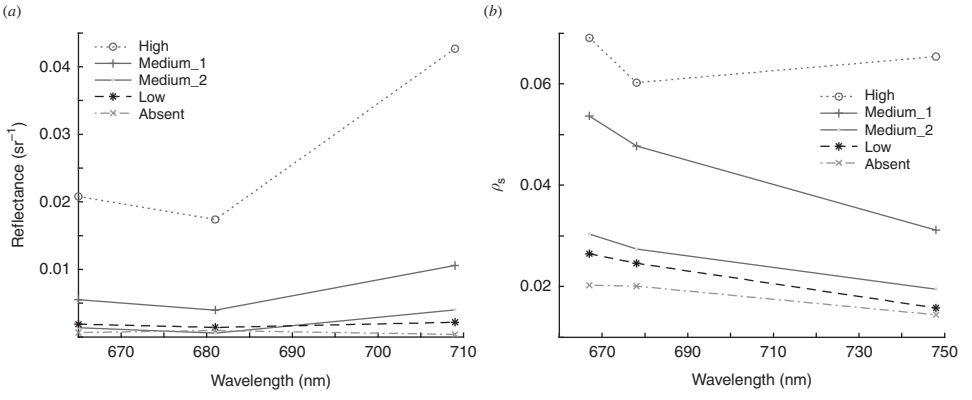

Figure 2. Spectra of the key bands for the CI_{MERIS} (*a*) and CI_{MODIS} (*b*) at high, medium, low, and absent cyanobacterial concentrations. These spectra were extracted from the image pair from 29 September 2010. The CI values (sr^{-1}) for MERIS from High, Medium_1 and Medium_2, Low, and Absent areas are: 0.011364, 0.00336, 0.00174, 0.00058, and –0.00387, respectively. The CI MODIS values are: 0.00835, 0.00290, 0.00144, 0.000432, and –0.000614, respectively.

especially when the central band (678 nm for MODIS, 681 nm for MERIS) is depressed relative to the adjacent shorter band (667 nm MODIS, 665 nm MERIS). Because the MODIS 754 nm band has inherently lower reflectance than the MERIS 709 nm band (owing to the greater absorption by water), there is less curvature for the MODIS bands, so MODIS would have a smaller CI relative to MERIS.

The years of 2008, 2009, and 2010 experienced intense blooms. 2011 experienced a tremendous bloom in cyanobacteria, perhaps the largest event in decades (Stumpf et al. 2012). Pairs of images acquired up to 1 day apart for each sensor were selected from the bloom season from these four years. Twenty-six image pairs were selected: ten from 2008, eight from 2009, four from 2010, and four from 2011 (Figures 3 and 4). Of these, 21 pairs had data from the same day. Imagery from 2007, a non-bloom year (Stumpf et al. 2012), did not record positive CI values in the lake for either sensor. This indicates that the CI_{MODIS} algorithm can be expected to respond only when cyanobacterial blooms are present during the summer bloom season.

A 3 × 3 median filter was applied to the CI products to reduce the influence of spatial discrepancies between the image pairs. The most fundamental are mapping discrepancies (nearest neighbour resampling is used, so any two 1 km areas on the ground may fall in two adjacent pixels), signal to noise limitations, including striping in the MODIS data, and the time difference between images. MERIS acquired data at approximately 10.00 local time, where MODIS Aqua acquires data at approximately 14.00 local time. Comparisons were made for pixels with a positive CI that were not flagged as clouds or land in both images. An additional condition was added to remove unreliable pixels from further analysis. This condition stipulated that MERIS $R(709)$ had to be greater than MERIS $R(754)$, removing pixels that were contaminated (or partially contaminated) with land, clouds, cloud shadow, glint, or surface scum. This reduced the number of pixels that were used for analysis in each MERIS image by an average of 2.96% (with a range between 0% and 10.79%).

To calculate a conversion factor so that CI_{MERIS} and CI_{MODIS} are comparable, a subset of four of the original 26 images was used. The image with the highest R^2 from each year was selected (Table 1). The selected images were acquired on the same day, having a reasonable number of pixels ($N > 250$) and high R^2 values (>0.5). Using the images

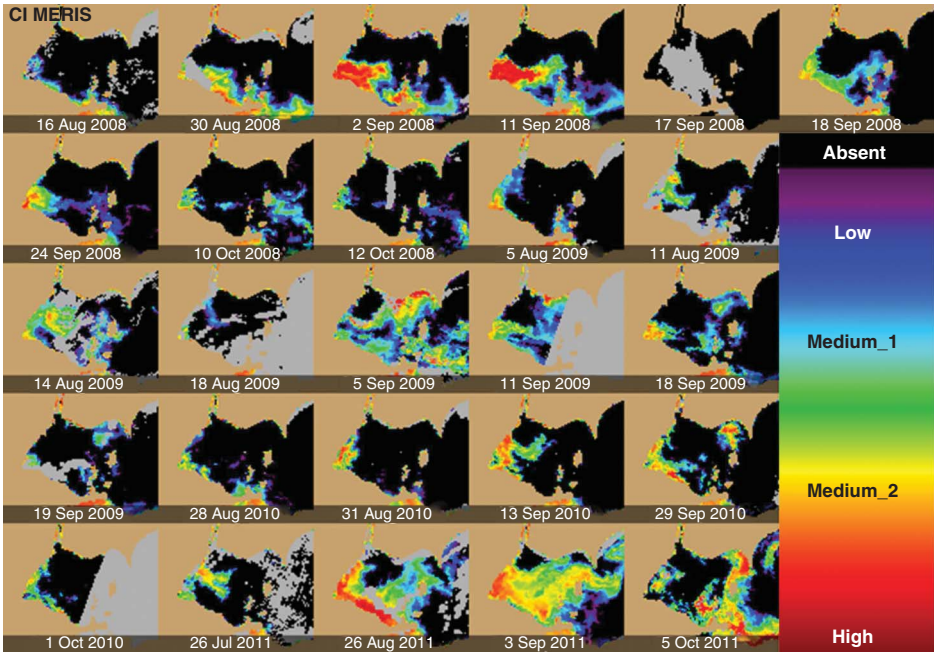

Figure 3. Time series of the CI_{MERIS}-derived imagery considered. The images are log scaled.

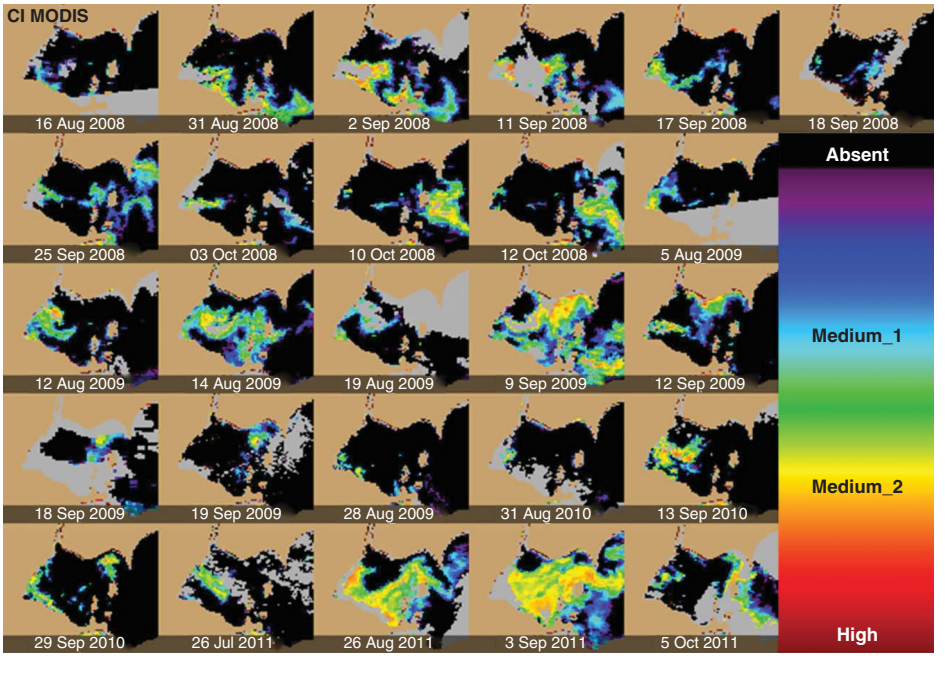

Figure 4. Time series of the CI_{MODIS}-derived imagery considered, with the same log scale as the CI_{MERIS} in Figure 3.

Table 1. Slopes, R^2, and p-values and the degrees of freedom (dF) from the images presented in Figures 2 and 3. Bold type indicates the image pairs that were used to create the scatter plots seen in Figure 5 and that were also used to derive the multiplier in Equation (5).

Image date MERIS	Image date MODIS	Slope	p-value	R^2	dF
16 Aug 2008	16 Aug 2008	1.3	$<2 \times 10^{-16}$	0.6100	74.00
30 Aug 2008	31 Aug 2008	1.1	$<2 \times 10^{-16}$	0.4100	782.0
02 Sep 2008	**02 Sep 2008**	**1.4**	$\mathbf{<2 \times 10^{-16}}$	**0.8000**	**962.0**
11 Sep 2008	11 Sep 2008	1.5	$<2 \times 10^{-16}$	0.5500	661.0
17 Sep 2008	17 Sep 2008	1.2	$<2 \times 10^{-16}$	0.7400	474.0
18 Sep 2008	18 Sep 2008	0.18	4×10^{-4}	0.0660	183.0
24 Sep 2008	25 Sep 2008	0.65	$<2 \times 10^{-16}$	0.3700	476.0
03 Oct 2008	03 Oct 2008	0.45	2×10^{-6}	0.2000	101.0
10 Oct 2008	10 Oct 2008	0.12	1×10^{-13}	0.1100	493.0
12 Oct 2008	12 Oct 2008	0.01	6×10^{-1}	0.0005	491.0
05 Aug 2009	**05 Aug 2009**	**1.6**	$\mathbf{<2 \times 10^{-16}}$	**0.7900**	**268.0**
11 Aug 2009	12 Aug 2009	0.59	$<2 \times 10^{-16}$	0.2900	300.0
14 Aug 2009	14 Aug 2009	0.90	$<2 \times 10^{-16}$	0.6000	832.0
18 Aug 2009	19 Aug 2009	0.59	2×10^{-3}	0.1900	44.00
05 Sep 2009	05 Sep 2009	0.79	$<2 \times 10^{-16}$	0.5100	1881
11 Sep 2009	12 Sep 2009	0.42	$<2 \times 10^{-16}$	0.4000	513.0
18 Sep 2009	18 Sep 2009	0.46	$<2 \times 10^{-16}$	0.5800	300.0
19 Sep 2009	19 Sep 2009	0.42	$<2 \times 10^{-16}$	0.6800	202.0
28 Aug 2010	28 Aug 2010	0.96	$<2 \times 10^{-16}$	0.5300	161.0
31 Aug 2010	31 Aug 2010	1.1	9×10^{-7}	0.4300	43.00
13 Sep 2010	13 Sep 2010	0.38	8×10^{-8}	0.0700	373.0
29 Sep 2010	**29 Sep 2010**	**1.5**	$\mathbf{<2 \times 10^{-16}}$	**0.5800**	**367.0**
26 Jul 2011	26 Jul 2011	0.89	1×10^{-15}	0.2400	232.0
26 Aug 2011	26 Aug 2011	1.1	$<2 \times 10^{-16}$	0.4500	1045
03 Sep 2011	**03 Sep 2011**	**0.91**	$\mathbf{<2 \times 10^{-16}}$	**0.7900**	**2017**
05 Oct 2011	05 Oct 2011	0.78	$<2 \times 10^{-16}$	0.2500	519.0

with the highest correlations will exclude any images that were overly dynamic in nature. Wynne et al. (2010, 2011) describe that under wind stress exceeding 0.1 Pa ($\sim$7.7 m s^{-1}) the biomass is mixed throughout the water column, while under calm conditions the cells return to the surface. Hunter et al. (2008) observed that concentrations may sometimes vary due to diurnal floating and sinking. In these situations, the 4 hour difference between the MERIS and MODIS Aqua overpasses may produce significant differences.

The bands on MODIS Aqua will saturate on bright targets including very turbid waters, precluding determination of the CI. The standard L2 cloud masking is perhaps overly conservative and will mask very turbid waters (in this case water with extremely high biomass of cyanobacteria) as clouds.

3. Results

The statistics from the CI_{MERIS} to CI_{MODIS} image pairs are summarized in Table 1. The four image pairs selected to determine a conversion of CI_{MODIS} to CI_{MERIS} were 2 September 2008, 5 August 2009, 29 September 2010, and 3 September 2011, each of which had the maximum R^2 value for its respective year (Figure 5). The average of the slopes obtained from these four image pairs was 1.3 +/– 0.3 (standard deviation). Slopes from pairs with

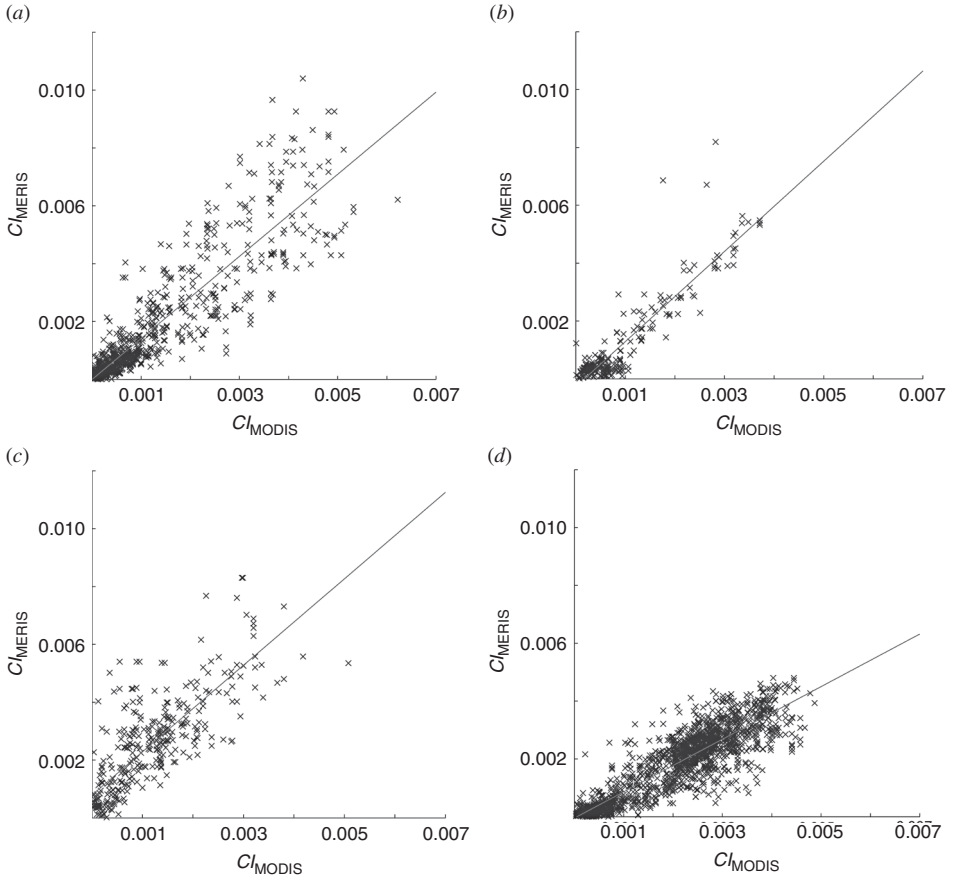

Figure 5. Regression of the four image pairs that had the highest correlation from (*a*) 2008, (*b*) 2009, (*c*) 2010, and (*d*) 2011.

low R^2 are not valid. (A regression of all points and imagery listed in Table 1 also had a slope of 1.3 +/− 0.3 (standard deviation).)

Therefore the following relationship can be deduced:

$$CI_{\mathrm{MODIS\_corr}} = CI_{\mathrm{MODIS}} \times 1.3, \tag{5}$$

where $CI_{\mathrm{MODIS\_corr}}$ is the MERIS CI approximated from the MODIS CI, and the multiplier, 1.3, has units of sr^{-1}. With this correction factor in place the time series of CI_{MODIS} was recalculated to $CI_{\mathrm{MODIS\_corr}}$ and can be seen in Figure 6.

The MODIS bands used to calculate the CI_{MODIS} (Equation (2)) can saturate. To illustrate this, Figure 7 shows the CI_{MERIS}, CI_{MODIS}, and true-colour MODIS from 2 September 2008, and 5 October 2011. The true-colour MODIS images were made from a composite of ρ_s (645), ρ_s (555), and ρ_s (469) and were from the high-resolution MODIS imagery (250 m). Much of the western portion of the bloom is masked as clouds by the L2 flags cloud algorithm in the 2 September image, where much of the eastern portion of the lake is saturated and masked as clouds in the 5 October image. These areas are consistent with

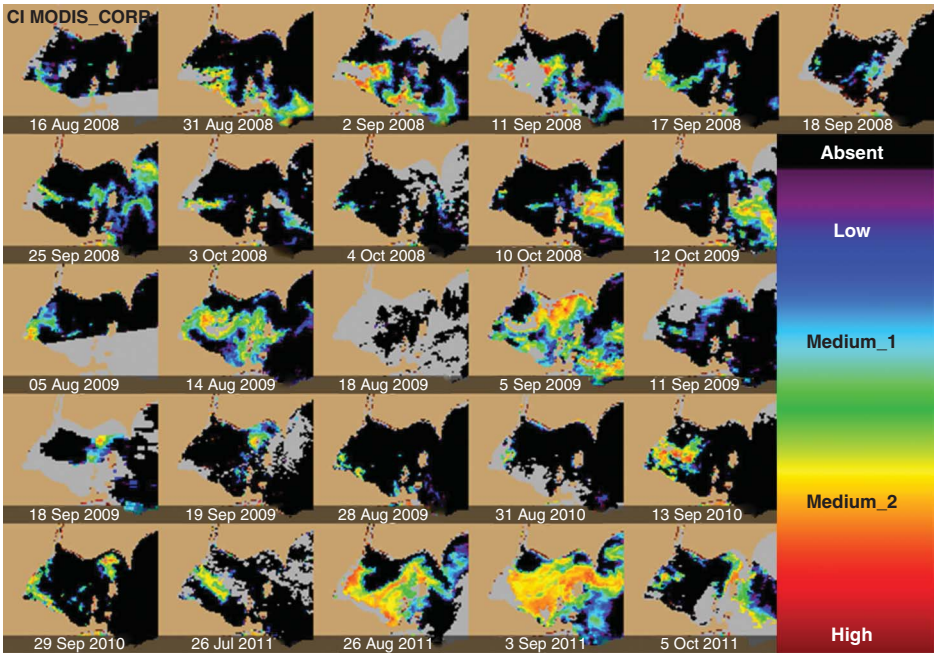

Figure 6. The time series of the corrected MODIS imagery ($CI_{\mathrm{MODIS\_corr}}$), these images being based on the imagery seen in Figure 4. These have been converted with the transform described later in the article and are logarithmic scaled the same as CI_{MERIS} in Figure 2.

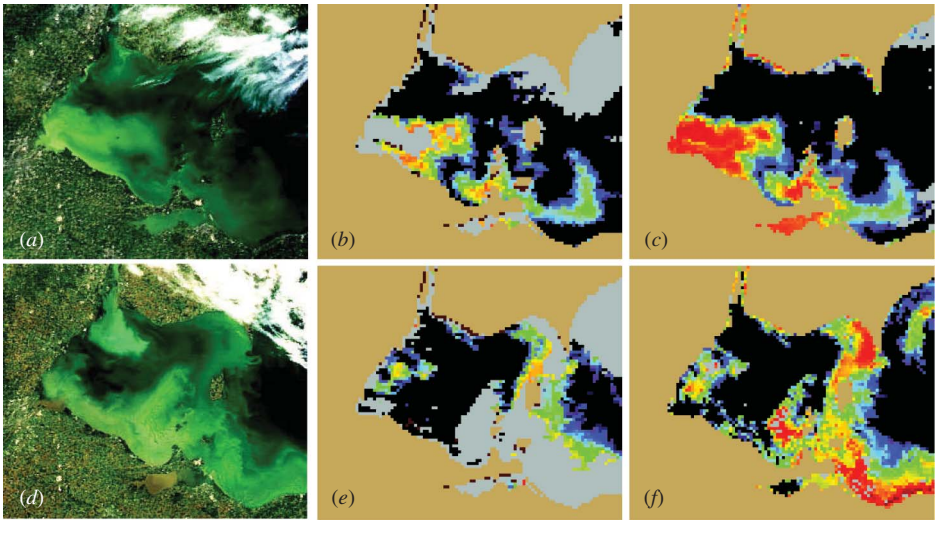

Figure 7. Figure (*a*)–(*c*) is from 2 September 2008 and shows the MODIS Aqua true-colour image, the CI_{MODIS}, and the CI_{MERIS}, respectively. Figures (*d*)–(*f*) are from the 5 October 2011 image and show the MODIS Aqua true colour, the CI_{MODIS}, and the CI_{MERIS}, respectively. Note that the true-colour images are free of clouds, and that the CI_{MODIS} is shown as clouds but the CI_{MERIS} is clear and unsaturated.

extremely high biomass of cyanobacteria and can cause a surface scum to occur on the water.

4. Discussion

The CI_{MODIS} identifies blooms that were found with CI_{MERIS}, with similar spatial patterns. A linear relationship (Equation (5)) allows estimation of the CI_{MERIS} from the CI_{MODIS}.

The spectral shape algorithms are robust. Gower, Doerffer, and Borstad (1999) developed spectral shape indices using top-of-atmosphere radiances for detection of blooms and floating algae. Stumpf and Werdell (2010) used the spectral shapes to track spectral drift in MODIS. Philpot (1991) showed how second derivatives are valid in the presence of atmospheric interference. This makes the derivative a powerful tool in coastal waters. Atmospheric correction algorithms in the presence of extremely turbid water, scum, or glint can depress the spectra sufficiently to lead to negative reflectance. Wynne et al. (2008, 2010) reported that over-correction for atmosphere can produce negative reflectance in 20% of the very turbid images in Lake Erie. While band ratio or semi-analytic algorithms will obviously fail under such conditions, a second derivative is computationally insensitive to poor or negligible atmospheric correction (Philpot 1991), as has been demonstrated in practice (Gower, Doerffer, and Borstad 1999; Hu, Lee, and Franz 2012; Wynne et al. 2008, 2010).

For each sensor, the overlap between the mid wavelength band (681 nm MERIS and 678 nm MODIS) and the red band (665 nm MERIS; 667 nm MODIS) may introduce some variations in the results for different backscatter and bloom intensities. The fact that the CI_{MERIS} imagery is calculated using R and the CI_{MODIS} imagery is calculated using ρ_{s} appears inconsequential when using the spectral shape algorithms. This is mostly due to the fact that in a spectral shape algorithm, such as that expressed in Equation (1), R and ρ_{s} are equivalent to one another. That is, the magnitudes may be different, but the patterns remain the same (Figure 2).

The residual variances between CIs in the image pairs will be influenced by several factors, including the timing difference between satellites and spatial heterogeneity. The 4 hour time difference could account for changes in surface concentration of the blooms – changes influenced by wind mixing. Wynne et al. (2010) showed that due to wind stress, surface concentrations of cyanobacteria change rapidly. It is possible that blooms with strong scattering will be detectable using this algorithm. For example, the spring chlorophyte bloom in Lake Erie has been flagged by the CI_{MERIS} algorithm.

As CI_{MODIS} is essentially the negative FLH, the standard (positive) FLH may fail as a bloom indicator in intense blooms in lakes and coastal waters. However, MODIS bands used for the CI_{MODIS} saturate with bright water (or aerosols), so the most extreme biomass concentrations may not be detected even using this algorithm. The results show that the MODIS FLH is not necessarily an indicator of intense blooms.

Several biophysical factors can produce the depression of the 678 nm (or 681 nm) band against the 667 nm (or 665 nm) band. Chlorophyll-*a* absorbs more strongly near 680 nm than near 665 nm (Bricaud et al. 1995), which would reduce the relative reflectance around 680 nm. Chlorophyll fluorescence may also be reduced. Fluorescence efficiency decreases with dense biomass. Huot, Brown, and Cullen (2005) suggested that a new term be added to the MODIS fluorescence product that accounts for the cellular reabsorption of fluoresced light. So it is possible that any fluoresced light is being reabsorbed by adjacent cells. This would further reduce reflectance around 680 nm. There is also evidence suggesting that cyanobacteria do not fluoresce as strongly as other types of algae (Seppälä et al. 2007).

The near-infrared reflectance increases with scattering. Ganf, Oliver, and Walsby (1989) estimated that the >80% of light scattering in natural populations of *Microcystis* were from the presence of gas vacuoles, which are not necessarily found in true algae. Potentially any strongly scattering dense phytoplantkon bloom that is near the surface may produce the same effect. This would mean that examination of the spectral shape other blooms is warranted.

Letelier and Abbott (1996); Hu et al. (2005); Moradi and Kabiri (2012) have used the MODIS FLH to look at oceanic productivity and delineate blooms of oceanic phytoplankton. The same bands in the CI_{MODIS} and CI_{MERIS} show that additional information can be obtained in cyanobacteria blooms, even when the fluorescence is not a factor (Seppälä et al. 2007). The results indicate that MODIS can provide a substitute for the MERIS for cyanobacterial bloom detection (Wynne et al. 2010, 2011, 2013 and Stumpf et al. 2012).

The results point to a new way to examine MODIS data and additional applications of spectral shape algorithms, especially for detection of dense algal blooms. This approach allows for the use of MODIS to continue the MERIS data set until the launch of Sentinel-3 with the OLCI, or to complement MERIS over the past 10 years.

Acknowledgements

MERIS imagery was provided by the European Space Agency (Category-1 Proposal C1P.3975). Funding was provided the NASA Applied Science Program announcement NNH08ZDA001N under contract NNH09AL53I.

References

Binding, C. E., T. A. Greenberg, and R. P. Bukata. 2011. "Time Series Analysis of Algal Blooms in Lake of the Woods Using MERIS Maximum Chlorophyll Index." *Journal of Plankton Research* 100: 13321–13332.

Bricaud, A., M. Babin, A. Morel, and H. Claustre. 1995. "Variability in the Chlorophyll-Specific Absorption Coefficients of Natural Phytoplankton: Analysis and Parameterization." *Journal of Geophysical Research* 100: 13321– 13332.

Brittain, S. M., J. Wang, L. Babcock-Jackson, W. W. Carmichael, K. L. Rinehart, and D. A. Culver. 2000. "Isolation and Characterization of Microcystins, Cyclic Hepatotoxins from Lake Erie Strains of *Microcystis Aeruginosa*." *Journal of Great Lakes Research* 26: 241–249.

Budd, J. W., A. Beeton, R. P. Stumpf, D. A. Culver, and W. C. Kerfoot. 2001. "Satellite Observations of Microcystis Blooms in Western Lake Erie." *Verhandlungen. Internationale Vereinigung fur Limnologie* 27: 3787–3793.

Ganf, G. G., R. L. Oliver, and A. E. Walsby. 1989. "Optical Properties of Gas-Vacuolate Cells and Colonies of *Microcystis* in Relation to Light Attenuation in a Turbid, Stratified Reservoir (Mount Bold Reservoir, South Australia)." *Australian Journal of Freshwater Research* 40: 595–611.

Gower, J., and S. King. 2007. "Validation of Chlorophyll Fluorescence Derived from MERIS on the West Coast of Canada." *International Journal of Remote Sensing* 28: 625–635.

Gower, J. F. R., R. Doerffer, and G. A. Borstad. 1999. "Interpretation of the 685 nm Peak in Water-Leaving Radiance Spectra in Terms of Fluorescence, Absorption, and Scattering and its Observation by MERIS." *International Journal of Remote Sensing* 20: 1771–1786.

Hu, C., Z. Lee, and B. Franz. 2012. "Chlorophyll A Algorithms for Oligotrophic Oceans: A Novel Approach Based on Three-Band Reflectance Difference." *Journal of Geophysical Research* 117: C01011.

Hu, C., F. E. Muller-Karger, C. Taylor, K. L. Carder, C. Kelble, E. Johns, and C. A. Heil. 2005. "Red Tide Detection and Tracing Using MODIS Fluorescence Data: A Regional Example in SW Florida Coastal Waters." *Remote Sensing of Environment* 97: 311–321.

Hunter, P. D., A. N. Tyler, N. J. Willby, and D. J. Gilvear. 2008. "The Spatial Dynamics of Vertical Migration by *Microcystis Aeruginosa* in a Eutrophic Shallow Lake: A Case Study Using High

Spatial Resolution Time-Series Airborne Remote Sensing." *Limnology and Oceanography* 53: 2391–2406.

Huot, Y., C. A. Brown, and J. J. Cullen. 2005. "New Algorithm for MODIS Sun-Induced Chlorophyll Fluorescence and a Comparison with Present Data Products." *Limnology and Oceanography: Methods* 3: 108–130.

Juhel, G., J. Davenport, J. O'Halloran, S. Culloty, R. Ramsey, K. James, A. Furey, and O. Allis. 2006. "Pseudodiarrhoea in Zebra Mussels *Dreissena Polymorpha* (Pallas) Exposed to Microcystins." *The Journal of Experimental Biology* 209: 810–816.

Kutser, T., L. Metsamaa, N. Strombeck, and E. Vahtmae. 2006. "Monitoring Syanobacterial Blooms by Satellite Remote Sensing." *Estuarine Coastal and Shelf Science* 67: 303–312.

Letelier, R. M., and M. R. Abbott. 1996. "An Analysis of Chlorophyll Fluorescence Algorithms for the Moderate Resolution Imaging Spectroradiometer (MODIS)." *Remote Sensing of Environment* 58: 215–223.

Lubac, B., H. Loisel, N. Guieselin, R. Astoreca, L. F. Artigas, and X. Mériaux. 2008. "Hyperspectral and Multispectral Ocean Color Inversions to Detect *Phaeocystis Globosa* Blooms in Coastal Waters." *Journal of Geophysical Research Oceans* 113: C06026.

Montagner, F. 2001. "Reference Model for MERIS Level 2 Processing." *European Space Agency*, document PO-TN-MEL-GS-0026.

Moradi, M., and K. Kabiri. 2012. "Red Tide Detection in the Strait of Hormuz (East of Persian Gulf) Using MODIS Fluorescence Data." *International Journal of Remote Sensing* 33: 1015–1028.

NASA. 2010. "l2gen." Accessed January 10, 2013. http://seadas.gsfc.nasa.gov/doc/l2gen/l2gen.html.

NASA. 2012. "OceanColor SeaDAS." Accessed January 10, 2013. http://seadas.gsfc.nasa.gov/.

Philpot, W. D. 1991. "The Derivative Ratio Algorithm: Avoiding Atmospheric Effects in Remote Sensing." *IEEE Transactions on Geoscience and Remote Sensing* 29: 350–357.

Ruiz-Verdú, A., S. G. H. Simis, C. de Hoyas, H. J. Gons, and R. Pena-Martinez. 2008. "An Evaluation of Algorithms for the Remote Sensing of Cyanobacterial Biomass." *Remote Sensing of Environment* 112: 3996–4008.

Seppälä, J., P. Ylöstalo, S. Kaitala, S. Hällfors, M. Raateoja, and P. Maunula. 2007. "Ship-Of-Opportunity Based Phycocyanin Fluorescence Monitoring of the Filamentous Cyanobacteria Bloom Dynamics in the Baltic Sea." *Estuarine Coastal and Shelf Science* 73: 489–500.

Shi, H., Q. Xing, C. Chen, P. Shi, and S. Tang. 2007. "Using Second-Derivative Spectrum to Estimate Chlorophyll-A Concentration in Turbid Estuarine Waters." In *Proceedings of SPIE, MIPPR 2007: Remote Sensing and GIS Data Processing and Applications*; and Innovative Multispectral Technology and Applications, edited by Y. Wang, J. Li, B. Lei, and J. Yang. Vol. 6790, 679032. doi:10.1117/12.747926.

Stumpf, R. P., and P. J. Werdell. 2010. "Adjustment of Ocean Color Sensor Calibration through Multi-Band Statistics." *Optics Express* 18: 401–412.

Stumpf, R. P., T. T. Wynne, D. B. Baker, and G. L. Fahnenstiel. 2012. "Interannual Variability of Cyanobacterial Blooms in Lake Erie." *PLoS One* 7: e42444.

Vanderploeg, H. A., J. R. Liebig, W. W. Carmichael, M. A. Agy, T. H. Johengen, G. L. Fahnenstiel, and T. F. Nalepa. 2001. "Zebra Mussel (*Dreissena Polymorpha*) Selective Filtration Promoted Toxic *Microcystis* Blooms in Saginaw Bay (Lake Huron) and Lake Erie." *Canadian Journal of Fisheries and Aquatic Sciences* 58: 1208–1221.

Wynne, T. T., R. P. Stumpf, M. C. Tomlinson, and J. Dyble. 2010. "Characterizing a Cyanobacterial bloom in Western Lake Erie Using Satellite Imagery and Meteorologic Data." *Limnology and Oceanography* 55: 2025–2036.

Wynne, T. T., R. P. Stumpf, M. C. Tomlinson, G. L. Fahnensteil, D. J. Schwab, J. Dyble, and S. Joshi. 2013. "Evolution of a Cyanobacterial Bloom Forecast System in Western Lake Erie: Development and Initial Evaluation." *Journal of Great Lakes Research*. http://dx.doi.org/10.1016/j.jglr.2012.10.003

Wynne, T. T., R. P. Stumpf, M. C. Tomlinson, D. J. Schwab, G. Y. Watabayashi, and J. D. Christensen. 2011. "Estimating Cyanobacterial Bloom Transport by Coupling Remotely Sensed Imagery and a Hydrodynamic Model." *Ecological Applications* 21: 2709–2721.

Wynne, T. T., R. P. Stumpf, M. C. Tomlinson, R. A. Warner, P. A. Tester, J. Dyble, and G. L. Fahnenstiel. 2008. "Relating Spectral Shape to Cyanobacterial Blooms in the Laurentian Great Lakes." *International Journal of Remote Sensing* 29: 3665–3672.